Asian Journal of Applied Science and Technology (AJAST)
Volume 7, Issue 3, Pages 213-223, July-September 2023

Evaluating Mica Shielding Effects in 2G Mobile Communication: Implications for SAR and Human Health

Amit Halder[1*], Mohammad Quamruzzaman[2], Md. Riyad Tanshen[3] & Md. Mohsin[4]

[1-4]Department of Electrical and Electronic Engineering, World University of Bangladesh, Dhaka-1230, Bangladesh.
*Corresponding Author (Amit Halder) Email: amit.rueten@gmail.com**

DOI: https://doi.org/10.38177/ajast.2023.7315

Article Received: 12 July 2023 *Article Accepted: 21 September 2023* *Article Published: 29 September 2023*

ABSTRACT

This research investigates the impact of 2G mobile communication signals on human well-being by employing numerical simulations to assess electromagnetic wave absorption and tissue heating within the human skull. Using COMSOL Multiphysics and solving the frequency domain nonhomogeneous electromagnetic wave equations, we calculate the Specific Absorption Rate (SAR) as a measure of energy absorption by the human body when exposed to 2G uplink (890 MHz to 915 MHz) and downlink (935 MHz to 960 MHz) frequencies. The novelty of this work lies in its comprehensive analysis of SAR with varying frequencies and Mica shielding sheet thicknesses, revealing a substantial increase in SAR values as frequency rises. This underscores the significance of material selection and thickness considerations in real-world scenarios involving 2G mobile communications. The SAR has undergone a remarkable reduction of 92.79% at the uplink operating frequency of 900 MHz and a corresponding reduction of 89.91% at the downlink operating frequency of 950 MHz. These findings provide valuable insights for researchers and policymakers concerned with the potential health effects of prolonged exposure to 2G signals, contributing to ongoing discussions regarding the influence of electromagnetic waves on human well-being.

Keywords: 2G mobile communication; Specific Absorption Rate (SAR); Mica shielding; Electromagnetic wave absorption; Numerical simulations.

1. Introduction

The rapid proliferation of mobile communication technologies has sparked ongoing debates and investigations into their potential impacts on human health [1]. Among these technologies, 2G mobile communication systems, operating at frequencies within the radio frequency (RF) spectrum, have been a subject of significant interest [2]. Understanding the interaction between electromagnetic waves emitted by 2G signals and the human body is critical for evaluating their implications for human well-being [3]. In this context, this research employs advanced numerical simulations to delve into the intricate dynamics of electromagnetic wave absorption and tissue heating within the human skull—a central area of concern for potential health effects [4]. Utilizing the powerful COMSOL Multiphysics platform and employing the solution of frequency domain nonhomogeneous electromagnetic wave equations, we conduct an in-depth assessment of Specific Absorption Rate (SAR). SAR quantifies the rate at which energy is absorbed by the human body when exposed to RF electromagnetic fields [5]. We focus our investigation on two crucial frequency bands: the uplink (890 MHz to 915 MHz) and downlink (935 MHz to 960 MHz) frequencies, corresponding to 2G mobile communication.

In the study conducted by Islam et al. (2009), the research focuses on reducing Specific Absorption Rate (SAR) in the human head using ferrite sheet attachments. They employ the finite-difference time-domain method with the Lossy-Drude model to investigate the impact of attachment location, distance, size, and material properties of ferrite sheets on SAR reduction. Computational findings reveal a substantial 57.75% reduction in SAR for a 10 gm average, offering valuable insights into optimizing ferrite sheet selection for minimizing SAR in phone models [6]. Apreutesei et al. (2016) conducted research into fabrics with metallic yarns, assessing their electromagnetic shielding properties and their potential to reduce mobile phone radiation from 2G and 3G communication

Asian Journal of Applied Science and Technology (AJAST)
Volume 7, Issue 3, Pages 213-223, July-September 2023

standards. Their findings highlighted the need to consider more than just shielding effectiveness when assessing protective materials due to complex interactions with mobile phone radiation, particularly regarding variations in energy absorption [7].

Chan and Soong (2016) introduced the discrete weighted centroid localization (dWCL) algorithm for wireless sensor networks, offering flexibility through node grouping and discrete weight assignment. Their research demonstrated the adaptability and optimization potential of dWCL, providing valuable insights for indoor positioning systems [8]. Miclăuş et al. (2017) explored the shielding efficiency of an amorphous ferromagnetic textile against dual-band mobile phone radiation (2G and 3G). Their study revealed substantial reductions in Specific Absorption Rate (SAR), with up to a 30% decrease for 2G technology and up to 24% for 3G technology. This emphasized the textile's potential to mitigate electromagnetic radiation effects from mobile devices, particularly in near-field conditions, with implications for human health and safety [9].

Halder et al. (2023) conducted research addressing the critical concern of radio frequency electromagnetic energy emitted by mobile phones and its impact on human well-being. They focused on measuring the Specific Absorption Rate (SAR) to quantify energy absorption within the human head. Using COMSOL Multiphysics, the study modeled SAR distribution and evaluated five different shielding materials, ultimately identifying a polyimide sheet as the most effective in aligning with ICNIRP guidelines for reducing electromagnetic radiation exposure. These findings have substantial implications for the mobile phone industry and public health, highlighting the significance of utilizing efficient shielding materials to mitigate radiation exposure [10]. The results of our study unveil significant patterns in SAR values as they relate to varying frequencies and the thickness of Mica shielding sheets—an important aspect of material selection for shielding against electromagnetic fields. A prominent finding reveals a substantial increase in SAR values with rising frequencies, particularly when thinner Mica shielding sheets are employed. This observation underscores the pivotal role of material selection and thickness considerations in real-world scenarios involving 2G mobile communication. Notably, we report a notable reduction in SAR values, amounting to 92.79% at the uplink frequency of 900 MHz and 89.91% at the downlink frequency of 950 MHz when effective shielding is implemented. These research findings have far-reaching implications for both the scientific community and policymakers engaged in discussions concerning the influence of electromagnetic waves on human well-being. They provide valuable insights into the potential health effects associated with prolonged exposure to 2G mobile communication signals and contribute substantively to the ongoing discourse in this critical field.

1.1. Research Objectives

The objectives of this research are to:

(a) Investigate the specific absorption rate (SAR) of 2G mobile communication signals in the frequency range of 890 MHz to 960 MHz, with a particular focus on the uplink (890 MHz to 915 MHz) and downlink (935 MHz to 960 MHz) frequencies.

(b) Assess the impact of varying frequencies on SAR values within the human skull to gain insights into the potential health risks associated with exposure to 2G signals.

(c) Analyze the influence of different Mica shielding sheet thicknesses on SAR values, highlighting the importance of material selection and thickness considerations in real-world scenarios.

(d) Quantify the reduction in SAR achieved at specific frequencies, such as 900 MHz and 950 MHz, to provide actionable information for researchers and policymakers concerned with minimizing health risks from prolonged 2G signal exposure.

(e) Contribute to the ongoing discussions regarding the potential effects of electromagnetic waves on human well-being and provide valuable data for informed decision-making in the field of mobile communication safety.

2. Design Methodology

The COMSOL software's symmetric human skull model is based on the requirements established by IEEE, IEC, and CENELEC for Specific Anthropomorphic Mannequin (SAM) Phantoms utilized for SAR (Specific Absorption Rate) measurements [11]. This model is based on an MRI picture with 109 slices comprising 256×256 voxels [12]. The final computer model faithfully mimics the physical dimensions of the head and consists of two separate components: one for the antenna and one for the head. A spherical geometry, which includes the surrounding air, is used to combine these components into a coherent computational domain.

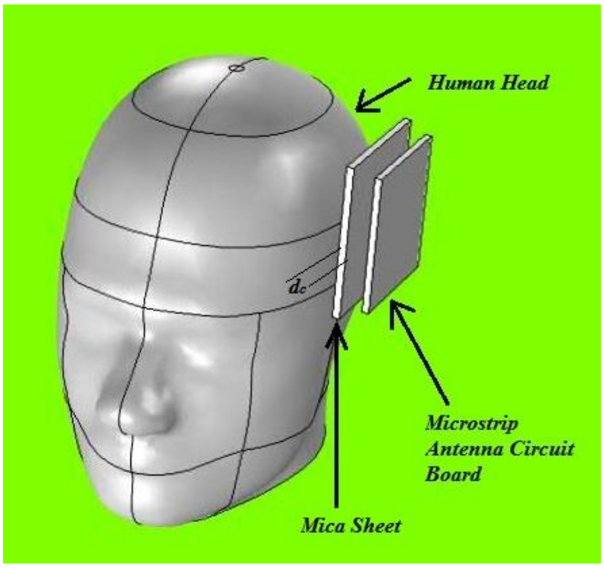

Figure 1. Side View of Three Dimensional Human Head Phantom Model with the Shielding Sheet and Radiating Antenna of a Mobile Phone

The patch antenna board is 8 cm long, 8 cm wide, and 4 mm thick, with a shielding material Mica sheet 9 cm long, 9 cm wide and d_c mm thick placed next to the human head model. Figure 1 illustrates the simulation configuration from the side. Mica is characterized by a relative permittivity (ε_r) of 6, indicating its ability to store electrical energy in an electric field. Its conductivity (σ) is quite low, with a value of 10^{-16} S/m, making it an excellent insulator with minimal electrical conduction capabilities. In terms of density (ρ), Mica has a value of 3100 kg/m³, denoting its relatively high mass per unit volume. These properties render Mica a suitable choice for electromagnetic shielding applications where the suppression of electrical conductivity is essential to prevent electromagnetic field penetration.

3. Simulation Method and Discussion

The influence of electromagnetic waves on human well-being remains a subject of ongoing investigation and debate. In the current study, the primary objective is to employ numerical simulations to assess the absorption of electromagnetic waves and the resulting tissue heating [13], thereby contributing to research efforts in this field. Specifically, we focus on the simulation of electromagnetic wave absorption stemming from cellphone usage and the subsequent temperature rise within the human skull, which encompasses various tissues such as skin-fat, bone, and brain tissues. COMSOL Multiphysics, equipped with vector elements in triangular and tetrahedral models, is employed for this purpose. The analysis of the electromagnetic field is executed by solving the frequency domain nonhomogeneous electromagnetic wave equations.

$$\nabla \times (1/\mu_r \nabla \times \overline{E}) - k_0^2[\varepsilon_r - \frac{i\sigma}{\omega\varepsilon_0}]\overline{E} = 0 \qquad (1)$$

The rate at which energy is taken up by the human body when exposed to a radio frequency (RF) electromagnetic field is quantified as the Specific Absorption Rate (SAR). Its formal definition is as follows [14]:

$$SAR = \frac{\sigma}{2\rho}\overline{E}^2 \quad \text{(W/kg)} \qquad (2)$$

Where σ represents the conductivity of body tissues (S/m), ρ denotes the density of body tissues (kg/m³), and E stands for the root mean square (RMS) value of the electric field strength within the tissue (V/m). It is important to note that SAR assessments are typically conducted for duration of 6 minutes, despite individuals often using mobile phones for extended periods, as documented in studies. The spatial average of the local exposure adhering to the general public SAR limit is stipulated at 2 W/kg over a 10g mass of tissues, in accordance with the standards established by the International Commission on Non-Ionizing Radiation Protection (ICNIRP) [15]. In order to ensure the preservation of human health and avoid adverse effects, SAR values must not surpass the designated threshold limits. The SAR Reduction Factor (SRF) is characterized as follows [16]:

$$SRF_{10g}(\%) = \frac{SAR_{10g} - SAR_{10g,s}}{SAR_{10g}} \times 100 \qquad (3)$$

Here, SRF_{10g} represents the SAR reduction factor for 10g peak SAR, where SAR_{10g} denotes the 10g peak SAR in the absence of shielding, and $SAR_{10g,s}$ signifies the 10g peak SAR when shielding is applied.

Table 1. Simulation Parameters

Material	Relative Permittivity, ϵ_r	Conductivity, σ (S/m)	Density, ρ (kg/m³)
Mica	6	10^{-16}	3100
Printed Circuit Board (PCB)	5.23	0.05	--
Brain Tissue	56	1.35	1030
Blood	61.4	1.54	1000

Asian Journal of Applied Science and Technology (AJAST)
Volume 7, Issue 3, Pages 213-223, July-September 2023

4. Computational Outcome and Discussions

Figure 2 illustrates the relationship between Specific Absorption Rate (SAR) values and frequency variations within the Uplink (Mobile to Base Station) frequency range, specifically spanning from 890 MHz to 915 MHz. The SAR values are evaluated for different thicknesses of Mica shielding sheets, starting with a thickness of 1.5 mm. For a 1.5 mm thickness, as the frequency increases from 890 MHz to 915 MHz, we observe a moderate increase in SAR values. These SAR values range from approximately 0.63 W/kg to 0.85 W/kg. When we increase the thickness to 2.5 mm while maintaining similar frequency variations, we continue to see an increase in SAR values, albeit at a slightly lower magnitude. Here, the SAR values range from around 0.38 W/kg to 0.51 W/kg, which is noticeably lower than the values observed for the 1.5 mm thickness. Now, when we consider a thinner shielding sheet with a thickness of 1 mm, the SAR values are significantly higher compared to the previous scenarios. They range from approximately 0.94 W/kg to 1.27 W/kg, indicating a more pronounced increase in SAR values with increasing frequency. This suggests a substantial rate of energy absorption, particularly at higher frequencies. On the contrary, when we increase the shielding thickness to 4.5 mm, it results in the lowest SAR values among the scenarios, ranging from about 0.13 W/kg to 0.16 W/kg. Although there is a slight increase in SAR values with frequency, this increase is the least prominent compared to the other scenarios. In summary, Figure 2 demonstrates that SAR values tend to increase as frequency rises, with variations depending on the thickness of the Mica shielding sheet. Thicker shielding sheets generally result in lower SAR values, while thinner sheets lead to higher SAR values, particularly at higher frequencies.

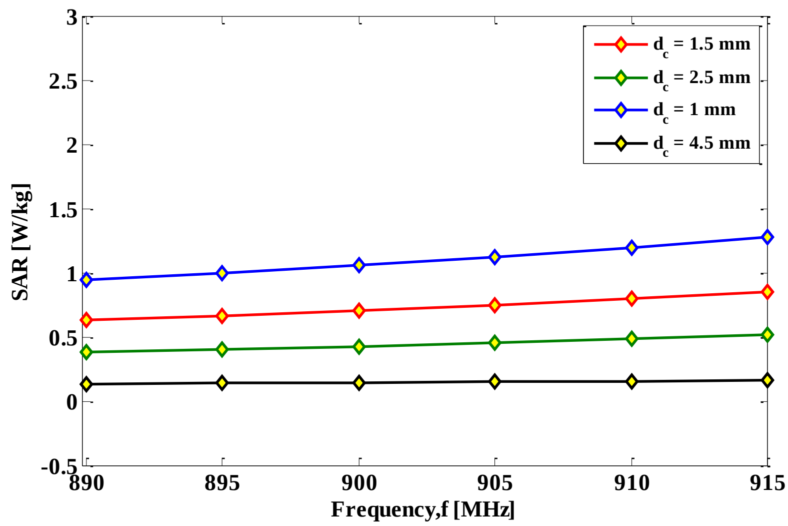

Figure 2. Plot Depicting How the Specific Absorption Rate (SAR) Varies with the Thickness of a Mica Sheet Across the Uplink Frequency Range (Mobile-to-Base Station)

Figure 3 explores how altering the thickness of Mica sheets influences SAR (Specific Absorption Rate) values across the downlink frequency spectrum, spanning from 935 MHz to 960 MHz. For the scenario with a 1.5 mm thick Mica sheet, SAR values consistently climb as frequency increases, ranging between 0.544827 W/kg and 0.635721 W/kg. Conversely, when using a 2.5 mm thick sheet, SAR values start lower at 0.327932 W/kg and peak at 0.382490 W/kg. Decreasing sheet thickness to 1 mm yields notably higher SAR values, commencing at 0.815743

Asian Journal of Applied Science and Technology (AJAST)
Volume 7, Issue 3, Pages 213-223, July-September 2023

W/kg and reaching a peak of 0.952049 W/kg, emphasize a substantial frequency-dependent escalation. In contrast, the 4.5 mm thickness scenario exhibits the lowest SAR values, initiating at 0.183652 W/kg and concluding at 0.213941 W/kg, indicating a modest rise with frequency. These findings underscore the pivotal role of material thickness in shaping SAR values at diverse frequencies, shedding light on the critical significance of material selection and thickness considerations in scenarios involving electromagnetic absorption. The results suggest that thinner sheets lead to higher SAR values, while thicker sheets result in lower SAR values. This nuanced relationship underscores the complexity of electromagnetic absorption and underscores the need for precise material choices in real-world applications.

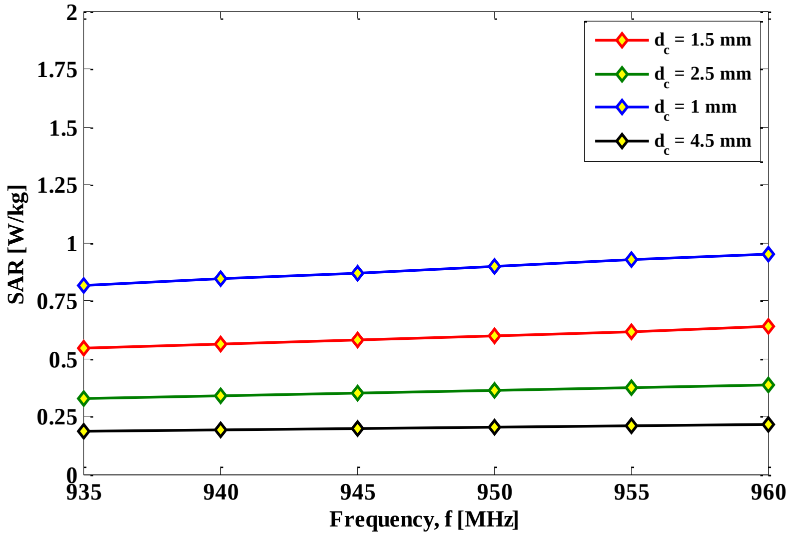

Figure 3. Plot Depicting How the Specific Absorption Rate (SAR) Varies with the Thickness of a Mica Sheet Across the Uplink Frequency Range (Base Station to Mobile Phone)

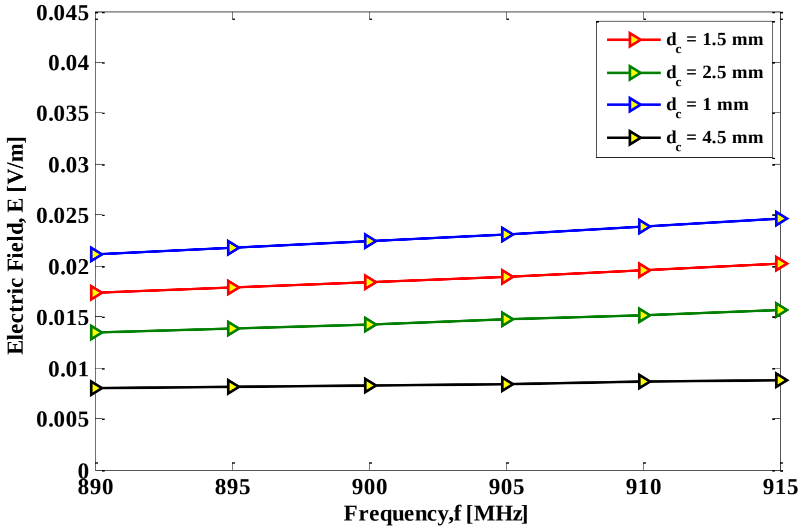

Figure 4. Electric Field Strength Variations (V/m) Across Different Thicknesses of Mica Shielding Sheets within the Uplink Frequency Spectrum (890 Mhz to 915 Mhz) for 2G Mobile Communication

Figure 4 illustrates the significant variations in electric field strength (in V/m) across different thicknesses of Mica shielding sheets within the uplink frequency range (890 MHz to 915 MHz) for 2G mobile communication. The data

underscores the crucial influence of shielding material thickness on tissue exposure to electromagnetic fields. Thinner 1 mm shielding sheets display substantially higher electric field strengths, ranging from 0.021182 V/m to 0.024662 V/m at 915 MHz, indicative of elevated tissue exposure. In contrast, thicker 4.5 mm sheets exhibit notably lower electric field strengths, with values spanning from 0.008022 V/m at 890 MHz to 0.008738 V/m at 915 MHz, emphasizing the effectiveness of thicker materials in minimizing tissue exposure.

Figure 5 presents a comprehensive view of electric field strength variations, measured in V/m, across different thicknesses of Mica shielding sheets in the downlink frequency spectrum (935 MHz to 960 MHz) for 2G mobile communication. The data vividly illustrates the pivotal role of shielding material thickness in determining tissue exposure to electromagnetic fields. For the thinnest 1 mm shielding sheet, electric field strengths range from 0.019744 V/m to 0.021330 V/m, indicating notably higher exposure levels. Conversely, increasing the thickness to 2.5 mm results in lower electric field strengths, spanning from 0.012519 V/m to 0.013520 V/m at 960 MHz, underscoring the shielding effectiveness of thicker materials. The thickest 4.5 mm shielding sheet exhibits the lowest electric field strengths, ranging from 0.009368 V/m to 0.010111 V/m, affirming the substantial reduction in tissue exposure. Additionally, the consistent upward trend of electric field strength with higher frequencies emphasizes the significance of frequency-dependent assessments in understanding the potential health implications of 2G mobile communication signals. These findings provide critical insights for assessing and managing electromagnetic field exposure, particularly in the context of 2G mobile communication, and highlight the importance of material thickness considerations in real-world scenarios.

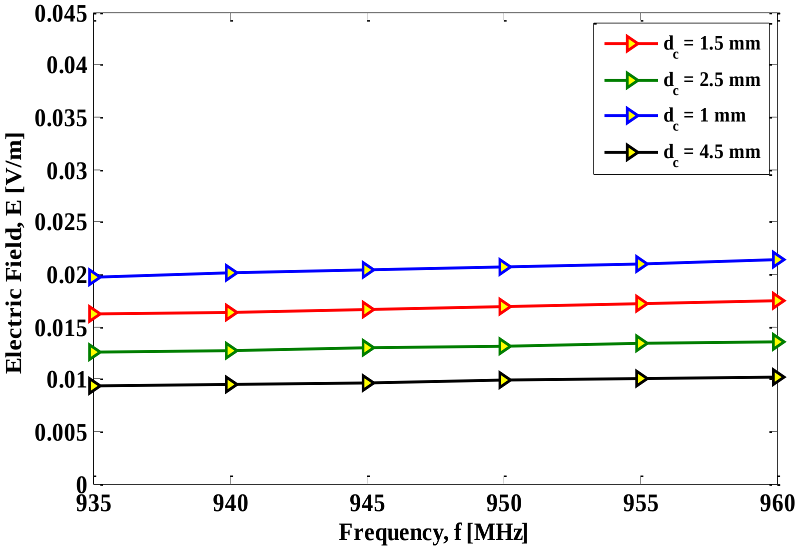

Figure 5. Electric Field Strength Variations (V/m) across Different Thicknesses of Mica Shielding Sheets within the Downlink Frequency Spectrum (935 Mhz to 960 Mhz) for 2G Mobile Communication

In Table 2 the Specific Absorption Rate (SAR) reduction factor achieved by Mica shielding at the operating frequencies of 900 MHz for the uplink scenario and 950 MHz for the downlink scenario. SAR is calculated for a 10g peak SAR, which aligns with the ICNIRP standard value for local exposure. The table presents results for varying thicknesses of Mica shielding sheets (ranging from 1 mm to 4.5 mm). For the uplink scenario, at 900 MHz, the SAR reduction factors range from 47.25% to 92.79%, indicating a substantial reduction in SAR values with

thicker shielding. Similarly, in the downlink scenario at 950 MHz, the SAR reduction factors span from 55.14% to 89.91%, further highlighting the shielding effectiveness of thicker Mica sheets. These findings underscore the critical role of Mica shielding thickness in mitigating SAR and thus reducing tissue exposure to electromagnetic fields in compliance with ICNIRP standards.

Table 2. SAR Reduction Factor for Mica Shielding at Operating Frequency for Uplink and Downlink Scenarios with Different Thicknesses

Uplink Operating Frequency = 900 MHz			
Thickness, d_c (mm)	**SAR without shielding for 10g peak SAR, SAR_{10g}** (ICNIRP standard value for local exposure) **W/kg**	**SAR with shielding for 10g peak SAR,** $SAR_{10g,s}$ **W/kg**	**SAR reduction factor for 10g peak SAR,** $SRF_{10g}(\%)$
1.5	2	0.705	64.75
2.5	2	0.4255	78.73
1	2	1.055	47.25
4.5	2	0.1442	92.79
Downlink Operating Frequency = 950 MHz			
Thickness, d_c (mm)	**SAR without shielding for 10g peak SAR,** SAR_{10g} (ICNIRP standard value for local exposure) **W/kg**	**SAR with shielding for 10g peak SAR,** $SAR_{10g,s}$ **W/kg**	**SAR reduction factor for 10g peak SAR,** $SRF_{10g}(\%)$
1.5	2	0.5992	70.04
2.5	2	0.3606	81.97
1	2	0.8972	55.14
4.5	2	0.2018	89.91

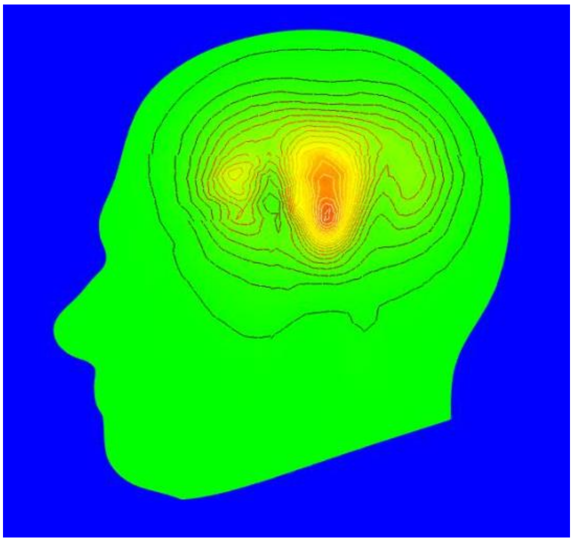

Figure 6. 2D Side View of Electromagnetic Field Distribution Contour Plot

Figure 6 presents a 2D side view of an electromagnetic field distribution contour plot. This visual representation provides a comprehensive depiction of how electromagnetic fields are distributed within a specific area or structure, typically within the context of a numerical simulation. The contour plot employs a color gradient to illustrate variations in electromagnetic field intensity, with different colors indicating different field strengths. In this specific plot, the focus is on the side view, which allows for an examination of how the electromagnetic field interacts with objects or materials from a lateral perspective. The contour lines, often referred to as isolines, connect points of equal field strength, creating a visual map of the field's behavior.

5. Conclusion and Future Recommendations

Compared to existing methods, our study provides a more comprehensive understanding of the relationship between SAR values, frequency, and shielding materials. By systematically analyzing SAR across a range of frequencies and varying shielding thicknesses, we offer valuable insights into the dynamic nature of electromagnetic wave absorption within the human skull. This nuanced perspective allows for a better-informed assessment of potential health risks associated with 2G mobile communication signals, taking into account real-world variability in signal conditions. In this study, we investigated the impact of 2G mobile communication signals on human well-being through numerical simulations assessing electromagnetic wave absorption and tissue heating within the human skull. Our results demonstrated a significant increase in Specific Absorption Rate (SAR) values with rising frequencies, particularly when thinner Mica shielding sheets were used. This highlights the crucial role of material selection and thickness in real-world scenarios involving 2G mobile communications, emphasizing the need for informed decision-making to mitigate potential health risks. For future research, we recommend exploring alternative shielding materials, extending exposure duration assessments, conducting multi-frequency analyses, performing health impact studies, advocating for updated regulations, and promoting public awareness of SAR values. These endeavors will contribute to a more comprehensive understanding of the implications of electromagnetic field exposure and support informed decision-making in the evolving landscape of wireless communication technology. In the realm of future research, several critical avenues beckon for a deeper understanding of the interplay between electromagnetic fields and human health. Firstly, the exploration of alternative shielding materials beyond Mica is imperative. Identifying materials that offer enhanced protection against electromagnetic wave absorption can lead to more effective shielding solutions and improved safety in our wireless world. Additionally, extending SAR assessments to longer durations, mirroring real-world mobile phone usage patterns, will yield a more precise assessment of potential health risks associated with prolonged exposure to 2G signals. Furthermore, conducting multi-frequency analyses, encompassing emerging communication technologies, will enable us to proactively anticipate health implications as wireless communication evolves. Complementing this, comprehensive health impact studies correlating SAR values with actual health outcomes will provide invaluable insights, painting a clearer picture of the potential risks to human well-being. Lastly, advocating for updated safety regulations that align with the latest research findings and the ever-evolving landscape of wireless communication technology is paramount to ensure the continued safety of the public. These collective endeavors will propel us toward a more informed and secure future in the domain of electromagnetic field exposure and its effects on human health.

Declarations

Source of Funding

This study did not receive any grant from funding agencies in the public or not-for-profit sectors.

Competing Interests Statement

The authors declare the total absence of conflicts of interest, both during the conduct of the study and during the written drafting of this work.

Consent for Publication

The authors declare that they consented to the publication of this research work.

Authors' Contributions

All the authors took part in literature review, analysis, and manuscript writing.

References

[1] Dang, S., Amin, O., Shihada, B., & Alouini, M.S. (2020). What should 6G be?. Nature Electronics, 3(1): 20–29. https://doi.org/10.1038/s41928-019-0355-6.

[2] Centenaro, M., Vangelista, L., Zanella, A., & Zorzi, M. (2016). Long-range communications in unlicensed bands: The rising stars in the IoT and smart city scenarios. IEEE Wireless Communications, 23(5): 60–67. https://doi.org/10.1109/MWC.2016.7721743.

[3] Narayanan, S.N., Jetti, R., Kesari, K.K., Kumar, R.S., Nayak, S.B., & Bhat, P.G. (2019). Radiofrequency electromagnetic radiation-induced behavioral changes and their possible basis. Environmental Science and Pollution Research, 26: 30693–30710. https://doi.org/10.1007/s11356-019-06278-5.

[4] Kainz, W., Neufeld, E., Bolch, W.E., Graff, C.G., Kim, C.H., Kuster, N., & Tsui, B.M. (2018). Advances in computational human phantoms and their applications in biomedical engineering–a topical review. IEEE transactions on radiation and plasma medical sciences, 3(1): 1–23. https://doi.org/10.1109/TRPMS.2018.2883437.

[5] Ali, M.F. (2017). Effects of non-ionizing electromagnetic radiation to the human body and environment. http://20.198.91.3:8080/jspui/bitstream/123456789/1643/1/Phd%20thesis%20%28ETCE%29%20Md.%20Faruk%20Ali.pdf

[6] Islam, M.T., Faruque, M.R.I., & Misran, N. (2009). Design analysis of ferrite sheet attachment for SAR reduction in human head. Progress in Electromagnetics Research, 98: 191–205. http://dx.doi.org/10.2528/PIER09082902.

[7] Apreutesei, A.L., Curteza, A., Paljanos, A., Miclaus, S., Bechet, P., Mihai, G., & Baltag, O. (2016). Radiation reduction capabilities of some woven fabrics with metallic yarns attached to mobile phones emitting in 2G-and 3G-communication standards. In 2016 International Conference and Exposition on Electrical and Power Engineering (EPE), Pages 387–391. https://doi.org/10.1109/ICEPE.2016.7781368.

[8] Chan, Y.W.E., & Soong, B.H. (2016). Discrete weighted centroid localization (dWCL): Performance analysis and optimization. IEEE Access, 4: 6283–6294. https://doi.org/10.1109/ACCESS.2016.2612225.

[9] Miclăuş, S., Mihai, G., Aron, A.M., Mitrescu, C., Bechet, P., & Baltag, O. (2017). Shielding efficiency of a fabric based on amorphous glass-covered magnetic microwires to radiation emitted by a mobile phone in 2G and 3G communication technologies. Land Forces Academy Review, 22(4): 289–297. https://sciendo.com/abstract/journals/raft/22/4/article-p289.xml.

[10] Halder, A., Quamruzzaman, M., Hossain, M.A., Mohsin, M., & Tanshen, M.R. (2023). Assessing Shielding Materials for Compliance with ICNIRP Recommendations Regarding Exposure to Electromagnetic Radiation from Mobile Devices. International Journal of Emerging Technologies and Innovative Research, Pages 2349–5162. https://papers.ssrn.com/sol3/papers.cfm?abstract_id=4413925.

[11] Dasi, S., Srinivas, Y., Vadivel, M., Satpathy, R., Dash, B.B., & De, U.C. (2022). Internet of Things (IoT) based Comprehensive testing of 5G network for Specific Absorption Rate (SAR). In 2022 International Conference on Electronics and Renewable Systems (ICEARS), Pages 506–510. https://doi.org/10.1016/j.compbiomed.2022.105277.

[12] Jabbarpour, A., Mahdavi, S.R., Sadr, A.V., Esmaili, G., Shiri, I., & Zaidi, H. (2022). Unsupervised pseudo CT generation using heterogenous multicentric CT/MR images and CycleGAN: Dosimetric assessment for 3D conformal radiotherapy. Computers in Biology and Medicine, 143: 105277. https://doi.org/10.1016/j.compbiomed.2022.105277.

[13] Abdul-Al, M., Amar, A.S., Elfergani, I., Littlehales, R., Ojaroudi Parchin, N., Al-Yasir, Y., & Abd-Alhameed, R.A. (2022). Wireless electromagnetic radiation assessment based on the specific absorption rate (SAR): A review case study. Electronics, 11(4): 511. https://doi.org/10.3390/electronics11040511.

[14] Turgut, A., & Engiz, B.K. (2023). Analyzing the SAR in Human Head Tissues under Different Exposure Scenarios. Applied Sciences, 13(12): 6971. https://doi.org/10.3390/app13126971.

[15] Davis, D., Birnbaum, L., Ben-Ishai, P., Taylor, H., Sears, M., Butler, T., & Scarato, T. (2023). Wireless technologies, non-ionizing electromagnetic fields and children: Identifying and reducing health risks. Current Problems in Pediatric and Adolescent Health Care, 101374. https://doi.org/10.1016/j.cppeds.2023.101374.

[16] Hediya, A., Attiya, A.M., & El-Deeb, W.S. (2022). Reduction of specific absorption rate: A review article. The Egyptian International Journal of Engineering Sciences and Technology, 39(3): 80–96. https://doi.org/10.21608/eijest.2022.108455.1117.